
This manuscript is a preprint and has not yet undergone peer-review. Subsequent versions of this manuscript may have different content. If accepted, the final version of this manuscript will be available via the '*Peer-reviewed Publication DOI*' link on the right-hand side of this webpage. Please feel free to contact any of the authors directly or to comment on the manuscript using **hypothes.is** (<https://web.hypothes.is/>). We welcome feedback!

1
2
3
4
5
6
7
8
9
10
11
12
13
14
15
16
17
18
19
20
21
22
23
24
25

**Magnetic stripes preserved in the continent-ocean transition zone offshore
NW Australia**

Matthew T. Reeve¹, Craig Magee^{1,2*}, Ian D. Bastow¹, Carl McDermott¹, Christopher A.-L. Jackson¹, Rebecca E. Bell¹, Julie Prytulak³

¹Basins Research Group (BRG), Department of Earth Science and Engineering, Royal School of Mines, Prince Consort Road, Imperial College London, SW7 2BP, England, UK.

²School of Earth and Environment, University of Leeds, Leeds, LS2 9JT, UK.

³Department of Earth Sciences, University of Durham, DH1 3LE, UK

*corresponding author: Craig Magee (c.magee@leeds.ac.uk)

Key Points

- 1) We identify seaward-dipping reflectors across the Cuvier Abyssal Plain and use chemical data to argue it is not oceanic crust as thought.
- 2) Magnetic stripes are thought unique to oceanic crust, but we show they can form in non-oceanic crust in continent-ocean transition zones.
- 3) We move the continent-ocean boundary of NW Australia oceanwards by >500 km.

26 **Abstract**

27 Magnetic stripes have long been used to define oceanic crust and the onset of submarine sea-
28 floor spreading. Identifying magnetic stripes is crucial for plate kinematic reconstructions,
29 and for estimating spreading rates and timing of continental break-up: the most landward
30 magnetic stripes are assumed to mark the oldest oceanic crust. However, continental crust
31 heavily intruded by magma during active sub-aerial rifting in Ethiopia, records magnetic
32 reversals akin to those observed in oceanic crust, implying magnetic stripes may not be
33 diagnostic of seafloor spreading. Recent work on South Atlantic volcanic passive margins has
34 identified linear magnetic anomalies within the continent-ocean transition zone (COTZ),
35 which is presently overlain by seaward dipping reflector (SDR) sequences of stacked lavas.
36 Perhaps surprisingly, magnetic stripes have rarely been observed in COTZ crust along
37 passive margins elsewhere. We use magnetic, 2D seismic reflection, and geochemical data to
38 examine the lithospheric structure of the Cuvier margin, offshore Northwest Australia, which
39 hosts well-defined, ≤ 220 km long magnetic stripe anomalies M10N–M5. Although
40 interpreted previously as oceanic crust, we suggest these magnetic stripes occur on a >500
41 km wide, Early Cretaceous COTZ. We suggest the magnetic anomalies record magnetic
42 reversal signatures originating from sheeted dykes and gabbroic intrusions within the sub-
43 SDR crust. Our interpretation implies the outer limit of Australia’s COTZ may thus be up to
44 >500 km further oceanward than previously recognised. Furthermore, this work strengthens a
45 growing consensus that magnetic reversals at rifted margins may not be truly diagnostic of
46 the onset of oceanic crust formation.

47

48 **Plain Text Summary**

49 Earth’s ocean floors are characterised by a barcode-like pattern of magnetic stripes parallel to
50 mid-ocean ridges. These stripes record reversals in Earth’s magnetic North and South field

51 when new rock was forming and moving away from submarine mid-ocean ridges; this is
52 fundamental evidence for continental drift and plate tectonic theory. Magnetic stripes have
53 long been considered unique to oceanic crust, but recent studies suggest they may form on
54 continental crust. We study the Cuvier Abyssal Plain offshore NW Australia, which displays
55 clear magnetic stripes and is thought comprise oceanic crust. We use seismic reflection data,
56 which provides ultrasound-like images of Earth's subsurface, to study the crusts structure and
57 show it contains thick sequences of lavas that were erupted in a sub-aerial environment. We
58 also reinterpret the chemistry of lavas from the proposed mid-ocean ridge that formed the
59 crust, and demonstrate the magma creating these rocks interacted with continental material.
60 Our evidence suggests the Cuvier Abyssal Plain is not formed of oceanic crust, but rather is a
61 hybrid of continental and oceanic crust. Our results mean that: (1) the continent-ocean
62 boundary of NW Australia could be >500 km further offshore; and (2) magnetic stripes may
63 not be diagnostic of oceanic crust.

64

65 **Index Terms**

66 1020; 1021; 1517; 8105; 8178

67

68 **Keywords**

69 Magnetic stripe; oceanic crust; continental crust; continent-ocean transition zone; seaward-
70 dipping reflectors; Australia

71

72

73 **1. Introduction**

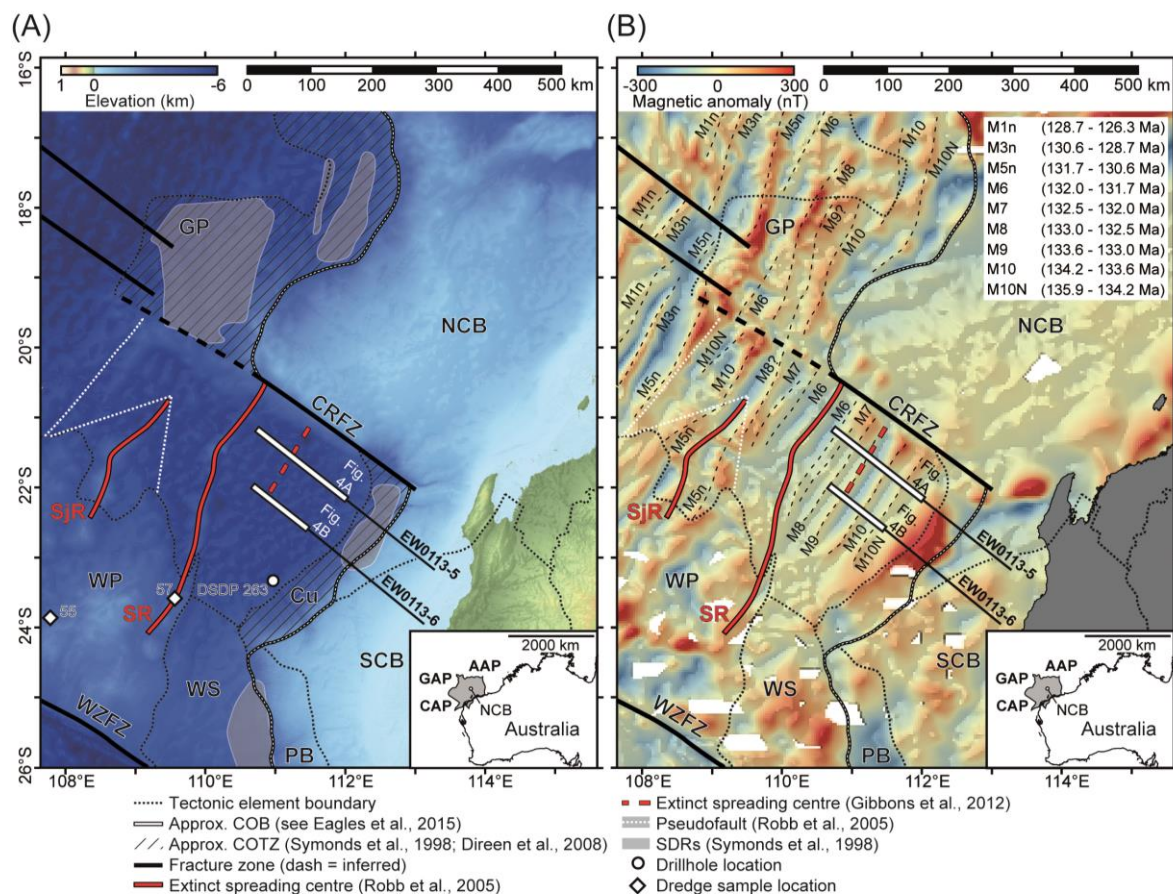
74 Development of magnetic reversal anomalies (stripes) during oceanic crust formation is
75 fundamental to modern plate tectonic theory (e.g., Vine & Matthews, 1963). Magnetic stripes

76 immediately adjacent to passive continental margins are commonly interpreted to mark a
77 basin's oldest oceanic crust, and have historically been used to define the continent-ocean
78 boundary (COB) (e.g., Eagles et al., 2015; Rabinowitz & LaBrecque, 1979; Talwani &
79 Eldholm, 1973; Veevers, 1986). Recognition and accurate mapping of COBs are critical to
80 palinspastic and plate kinematic reconstructions (e.g., Eagles et al., 2015). However,
81 improved long-offset seismic reflection and refraction data reveal continental break-up can
82 produce complex crustal domains up to several hundred kilometres wide, i.e. the continent-
83 ocean transition zone (COTZ), characterised by localized lithospheric thinning and
84 occasional mantle exhumation (see Eagles et al., 2015 and references therein). Uncertainties
85 in data resolution and interpretation make ascertaining the nature of COTZ crust challenging,
86 meaning it is difficult to uniquely define COBs (e.g., Eagles et al., 2015). Furthermore, linear
87 magnetic stripes have recently been identified: (i) in heavily intruded, transitional continental
88 crust of the onshore Afar Rift, Ethiopia (Bridges et al., 2012), which is expected to form part
89 of a COTZ assuming full lithospheric rupture occurs; (ii) along the COTZ offshore Iberia-
90 Newfoundland non-volcanic passive margin, recorded by intrusion of magma into exhumed
91 and serpentinised mantle prior to break-up (Bronner et al., 2011); (iii) within part of the
92 volcanic passive margin COTZ offshore NW Australia (i.e. the Gascoyne margin; Direen et
93 al., 2008); and (iv) in magmatic crust, which is wholly comprised of new igneous material
94 but formed during sub-aerial spreading (i.e. not oceanic crust), offshore South America
95 (Collier et al., 2017; McDermott et al., 2018). Given magnetic stripes can seemingly develop
96 within non-oceanic crust, these observations question whether magnetic stripes can be used to
97 diagnose seafloor spreading and COBs (Rooney et al., 2014).

98 The Cuvier margin, offshore NW Australia is an ideal location to explore the
99 development of magnetic stripes during the transition to seafloor spreading: it has well-
100 developed magnetic anomalies, calibrated to the global geomagnetic timescale (Robb et al.,

101 2005), and reflection and refraction seismic data capable of imaging the margin's deep
102 crustal structure. Previous seismic refraction and magnetic studies suggest the Cuvier
103 Abyssal Plain (CAP) is underlain by unambiguous oceanic crust, formed by submarine
104 spreading; this interpretation is based on the presence of magnetic stripes distributed about an
105 inferred submarine spreading centre along the Sonne Ridge (Fig. 1) (e.g., Falvey & Veevers,
106 1974; Larson et al., 1979; MacLeod et al., 2017; Robb et al., 2005). Basalts dredged from the
107 Sonne Ridge are interpreted to have an enriched MORB-like chemistry, supporting the
108 inference that the CAP comprises oceanic crust (Crawford & von Rad, 1994; Dadd et al.,
109 2015). Our concurrent analysis of magnetic and 2D seismic reflection data, coupled with an
110 examination of published chemical data, suggest the well-defined magnetic stripes of the
111 CAP actually occur within the COTZ. In particular, we recognise multiple packages of up to
112 ~3 km thick seaward-dipping reflector (SDR) sequences, which can extend across several
113 defined linear magnetic anomalies, imaged in seismic reflection data spanning ~200 km of
114 the CAP. Furthermore, reinterpretation of chemical data indicates basalts from the Sonne
115 Ridge, interpreted to be an abandoned submarine spreading centre (e.g., MacLeod et al.,
116 2017; Robb et al., 2005), contain a continental signature. Based on these observations and
117 data, we propose the CAP may not be oceanic crust and is instead representative of a COTZ
118 with an outer-limit >500 km oceanwards from where it is currently defined. Our
119 interpretation has important implications for plate reconstructions and heat flow and basin
120 modelling of the NW Australian margin. Furthermore, we argue that magnetic stripes may
121 not be a unique feature of oceanic crust.

122



123

124 Figure 1: (A) Location map of the study area highlighting key tectonic elements, including
 125 areas of recognised seaward-dipping reflectors (SDRs) (Holford et al., 2013; Symonds et al.,
 126 1998) and previously interpreted approximate (approx.) limits of the continent-ocean
 127 boundary (COB; Eagles et al., 2015) and continent-ocean transition zones (COTZs; Direen et
 128 al., 2008; Symonds et al., 1998). Inset: study area location offshore NW Australia. AAP –
 129 Argo Abyssal Plain, CAP – Cuvier Abyssal Plain, CRFZ – Cape Range Fracture Zone, GAP
 130 – Gascoyne Abyssal Plain, GP – Gallah Province, NCB – North Carnarvon Basin, SCB –
 131 South Carnarvon Basin, Cu – Cuvier margin COTZ, SR – Sonne Ridge, SjrR – Sonja Ridge,
 132 WP – Wallaby Plateau, WS – Wallaby Saddle, WZfZ – Wallaby-Zenith Fracture Zone.

133 Dredge sites 55 (samples 055BS004A and 055BS004B) and 57 (sample 057DR051A) are

134 also shown (Dadd et al., 2015). (B) Total magnetic intensity grid (EMAG2v2), interpreted

135 magnetic chrons (based on Robb et al., 2005). See Supplementary Figure S1 for an
136 uninterpreted version.

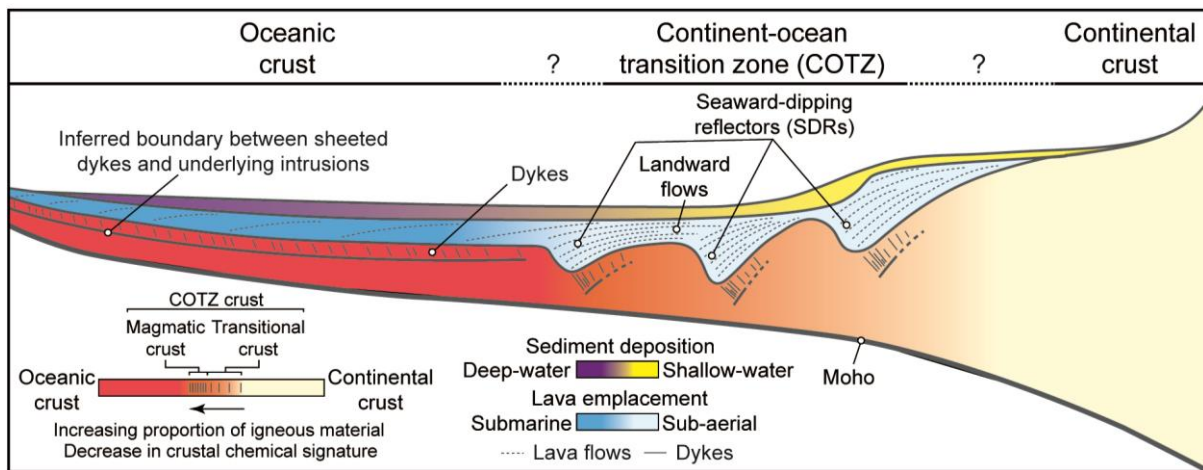
137

138 **2. Definitions**

139 We define a COTZ as the crustal domain separating unambiguous continental crust and
140 unambiguous normal oceanic crust (Eagles et al., 2015). Along volcanic or magma-rich
141 passive margins, COTZ's commonly comprise seismically isotropic, fast ($>7 \text{ km s}^{-1}$) crust,
142 overlain by SDR sequences of sub-aerially erupted, mafic volcanic products (e.g. lava flows)
143 interbedded with terrestrial sedimentary rocks (e.g., Eldholm et al., 1989; Larsen & Saunders,
144 1998; Menzies et al., 2002; Symonds et al., 1998). These SDR-bearing domains have been
145 further sub-divided into: (i) 'transitional crust', i.e. stretched and heavily intruded continental
146 crust (e.g., Eldholm et al., 1989); (ii) or 'magmatic crust' (also termed 'igneous' crust), which
147 effectively is structurally the same as oceanic crust but instead formed by sub-aerial, rather
148 than submarine, spreading (e.g., Collier et al., 2017; McDermott et al., 2018; Paton et al.,
149 2017). Where we can study active continental break-up and development of a possible future
150 COTZ in Ethiopia, the latter phases of rifting (i.e. prior to rupture) involve localisation of
151 extension into narrow zones (~20 km wide) dominated by dyke intrusion (e.g., Ebinger &
152 Casey, 2001; Keranen et al., 2004; Mackenzie et al., 2005; Maguire et al., 2006).
153 Observations from rifted margins and active rifts therefore suggest the COTZ at volcanic
154 passive margins is marked by a compositional and structural spectrum some way between
155 continental and oceanic end-members (Fig. 2). From their landward limit, at the age which
156 corresponds to onset of COTZ development, we expect the proportion of intruded material to
157 continental crust (i.e. transitional crust) to increase oceanwards, until no or very little
158 continental crust remains and the COTZ comprises igneous intrusions and extrusions formed
159 in sub-aerial spreading centres (i.e. magmatic crust) (Fig. 2). Given the localisation of dyking

160 within narrow zones we may expect an oceanwards reduction in the continental signature of
 161 magma chemistry as they become more MORB-like (Fig. 2). Because uncertainties in data
 162 resolution and interpretation mean we cannot identify a distinct boundary between
 163 transitional or magmatic crust (cf. Eagles et al., 2015), we henceforth combine these domains
 164 and refer to them both simply as ‘COTZ crust’ (Fig. 2).

165



166

167

168 Figure 2: Schematic model (not to scale) of a continent-ocean transition zone along a
 169 volcanic passive margin; for simplicity the lithospheric mantle is not shown. As magma
 170 intrudes continental crust, likely as dykes at mid- to upper-crustal levels and larger gabbroic
 171 bodies in the lower crust, it becomes ‘transitional crust’ (e.g., Eldholm et al., 1989).
 172 Continued intrusion and dyking leads to localisation of magmatism within narrow zones
 173 where sub-aerial spreading dominates extension and there is little, if any, continental crust
 174 remaining (i.e. magmatic crust) (i.e. ‘magmatic crust’; e.g., Collier et al., 2017; Paton et al.,
 175 2017). We categorize transitional and magmatic crust as ‘COTZ crust’. Sub-aerial spreading
 176 centres may feed extensive lava flows that later, through subsidence, become seaward-
 177 dipping reflectors (SDRs); SDR subsidence leads to rotation of underlying dykes

178 (Abdelmalak et al., 2015). A similar rotation of lavas and dykes is observed in oceanic crust
179 (Karson, 2019).

180

181 **3. Geological Setting**

182 The North Carnarvon Basin forms the southernmost part of the NW Australian volcanic
183 passive margin, bound by the Argo Abyssal Plain to the north, and the Gascoyne Abyssal
184 Plain and CAP to the west (Fig. 1) (Longley et al., 2002; Stagg et al., 2004). Basin formation
185 occurred during multiple phases of Permian-to-Late Jurassic rifting, culminating in Early
186 Cretaceous break-up of the Gascoyne and Cuvier margin rift segments (Longley et al., 2002).
187 We sub-divide the basin into the ~400 km wide Gascoyne and 180 km-wide Cuvier margin
188 sectors, separated by the NW-trending Cape Range Fracture Zone (Fig. 1). A 200–250 km
189 wide COTZ adjacent to the Gascoyne margin (i.e. the Gallah Province), comprises 2–5.5 km
190 thick SDRs and high-velocity lower crust formed during magnetic anomalies M10N–M5n
191 (i.e. ~136–131 Ma), with interpreted normal oceanic crust emplaced from chron M3r (~130
192 Ma) onwards (Fig. 1) (Direen et al., 2008). Seismic reflection data reveal SDR sequences
193 along the Cuvier margin, beneath the continental slope, within a previously interpreted 50–70
194 km wide COTZ (Fig. 1) (Hopper et al., 1992; Symonds et al., 1998). The CAP is partly
195 bound to the SW by the Wallaby Plateau (Fig. 1), a large bathymetric high likely comprising
196 thinned continental crust overlain by volcanic and sedimentary rocks (e.g., Colwell et al.,
197 1994; Daniell et al., 2009; Olierook et al., 2015; Stilwell et al., 2012).

198 The CAP lies ~5 km below sea level and comprises a 1–3.3 km thick sedimentary
199 sequence overlying 6–10.5 km thick crystalline crust, inferred to be oceanic in origin due to
200 the recognition of chrons M10N–M5 (Fig. 1B) (Falvey & Veevers, 1974; Larson et al.,
201 1979). The ~175 km long Sonne Ridge and ~100 km long Sonja Ridge, which bisect the CAP
202 and extend into the Wallaby Plateau (Fig. 1), are interpreted as probable extinct oceanic

203 spreading ridges (e.g., MacLeod et al., 2017; Mihut & Müller, 1998; Robb et al., 2005). The
204 Sonne Ridge has also been interpreted as a pseudofault (i.e. an apparent offset in magnetic
205 stripes formed by ridge jumps; Hey, 1977), based on changes in gravity intensity across it and
206 termination of the Cape Range Fracture Zone directly north of the ridge (Gibbons et al.,
207 2012). In their model, Gibbons et al. (2012) define a new spreading centre ~100 km to the SE
208 and parallel to the Sonne Ridge (Fig. 1). However, Gibbons et al. (2012) use the COB of
209 Heine and Müller (2005) to define the termination of the Cape Range Fracture Zone, but this
210 model does not account for the Gallah Province being part of the Gascoyne COTZ and,
211 hence, the required north-westward extension of the fracture zone (Direen et al., 2008; Robb
212 et al., 2005). We therefore favour and use the interpreted magnetic chron configuration of
213 Robb et al. (2005), centred on the Sonne Ridge, which predicts half-spreading rates adjacent
214 to both Gascoyne and Cuvier segments were similar during chrons M10-M5 (~4.5 cm/yr),
215 decreasing to ~3 cm/yr by chron M3.

216

217 **4. Dataset and methodology**

218 4.1. Seismic reflection data

219 We constrain the lithospheric structure of Cuvier margin COTZ using pre-stack time-
220 migrated seismic reflection and OBS-derived velocity data from the EW0113 survey. The
221 seismic reflection survey was acquired in 2001 by the R/V *Maurice Ewing* using an 8445 in³
222 airgun array and a 6 km streamer length (Tischer, 2006). Due to extreme amplitude contrasts
223 between the shallow and deep sections of the original migrated data, a time-dependent gain
224 filter and root filter were applied to improve amplitude balance and enhance deep reflectivity
225 (see supplementary information for details). Depth conversion of the seismic data was
226 performed using a velocity model based on velocities interpreted from OBS data by Tischer
227 (2006). The OBS array was co-located with seismic line EW0113-6, which is located ~70 km

228 along-strike from line EW0113-5 (Fig. 1). Each line is >300 km long and extends up to ~200
229 km out into the CAP from the currently defined COTZ, nearly reaching the Sonne Ridge
230 (Fig. 1).

231

232 4.2. Magnetic data

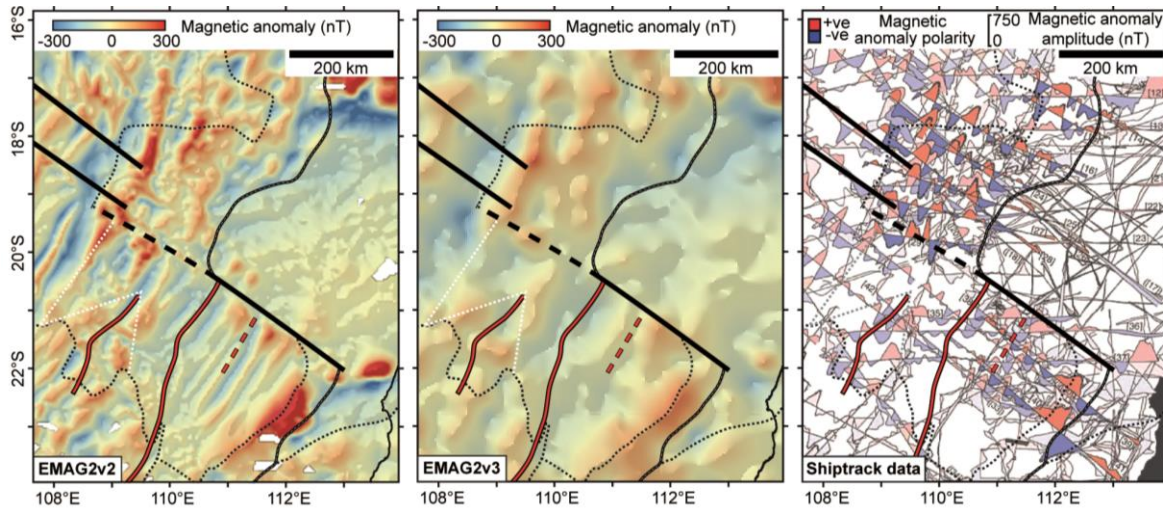
233 To examine the regional magnetic anomalies, we utilise the EMAG2v2 and EMAG2v3 Earth
234 Magnetic Anomaly Grids (Maus et al., 2009; Meyer et al., 2017). EMAG2v2 is a 2 arc min
235 resolution grid derived from marine, airborne, and satellite magnetic data, but uses a priori
236 information to interpolate magnetic anomalies in areas where data gaps are present (Fig. 3)
237 (Maus et al., 2009; Meyer et al., 2017). In contrast, EMAG2v3 uses more data points to
238 derive magnetic anomaly maps but assumes no a priori information (Fig. 3) (Meyer et al.,
239 2017). In ocean basins with a relatively poor coverage of magnetic data available, such as the
240 CAP, clear linear magnetic anomalies in EMAG2v2 thus typically appear poorly developed
241 or are absent in EMAG2v3 (Fig. 3) (Meyer et al., 2017). This difference in the presence and
242 appearance of linear magnetic anomalies between the EMAG2v2 and EMAG2v3 grids is
243 because knowledge of seafloor spreading processes was incorporated into, and therefore
244 influenced, interpolation during construction of the EMAG2v2 grid (Maus et al., 2009;
245 Meyer et al., 2017). Importantly, the apparent reduction in magnetic stripes observed in
246 EMAG2v3, compared to EMAG2v2 (Fig. 3), does not necessarily mean these features are
247 absent, but rather that the available data is insufficient to unambiguously confirm their
248 presence (Meyer et al., 2017). Comparing the EMAG2v2 and EMAG2v3 grids, coupled with
249 shiptrack magnetic data (Robb et al., 2005), allows us to interrogate the magnetic architecture
250 of the CAP (cf. Meyer et al., 2017). In particular, we use EMAG2v2 to interpret possible
251 magnetic chrons, picked on positive peaks (Fig. 1), and attempt to correlate them to the
252 EMAG2v3 grid and shiptrack magnetic data. From these comparisons, we tied interpreted

253 magnetic stripes to seismic line EW0113-5 using the synthetic profiles of Robb et al. (2005).

254 We use the magnetic polarity reversal sequence and absolute ages of Gradstein and Ogg

255 (2012).

256



257

258

259 Figure 3: Total magnetic intensity grids EMAG2v2 and EMAG2v3 (Maus et al., 2009; Meyer

260 et al., 2017), compared with shiptrack magnetic data (Robb et al., 2005). Key tectonic

261 elements also shown (see Fig. 1 for legend).

262

263 4.3. Geochemical data

264 To evaluate whether the Sonne Ridge is an extinct seafloor spreading centre (e.g., Mihut &

265 Müller, 1998; Robb et al., 2005), which implies it consists of oceanic crust with a MORB or

266 MORB-like affinity along its length, we examine chemical data for a Sonne Ridge basalt lava

267 sample (i.e. sample 057DR051A; Dadd et al., 2015). The analysed sample was dredged from

268 the south-western section of the Sonne Ridge, where it bounds the south-eastern extent of the

269 Wallaby Plateau (Dadd et al., 2015; Daniell et al., 2009; Olierook et al., 2015). We compare

270 the Sonne Ridge sample to two collected from within the Wallaby Plateau (i.e. samples

271 055BS004A and 055BS004B), towards its south-western margin (Dadd et al., 2015). The two

272 Wallaby Plateau basalts yield plagioclase $^{40}\text{Ar}/^{39}\text{Ar}$ plateau ages of 125.12 ± 0.9 Ma and
273 123.80 ± 1.0 Ma, whilst two analyses of the Sonne Ridge sample yielded less precise ages of
274 120 ± 14 Ma and 123 ± 11 Ma (Olierook et al., 2015).

275

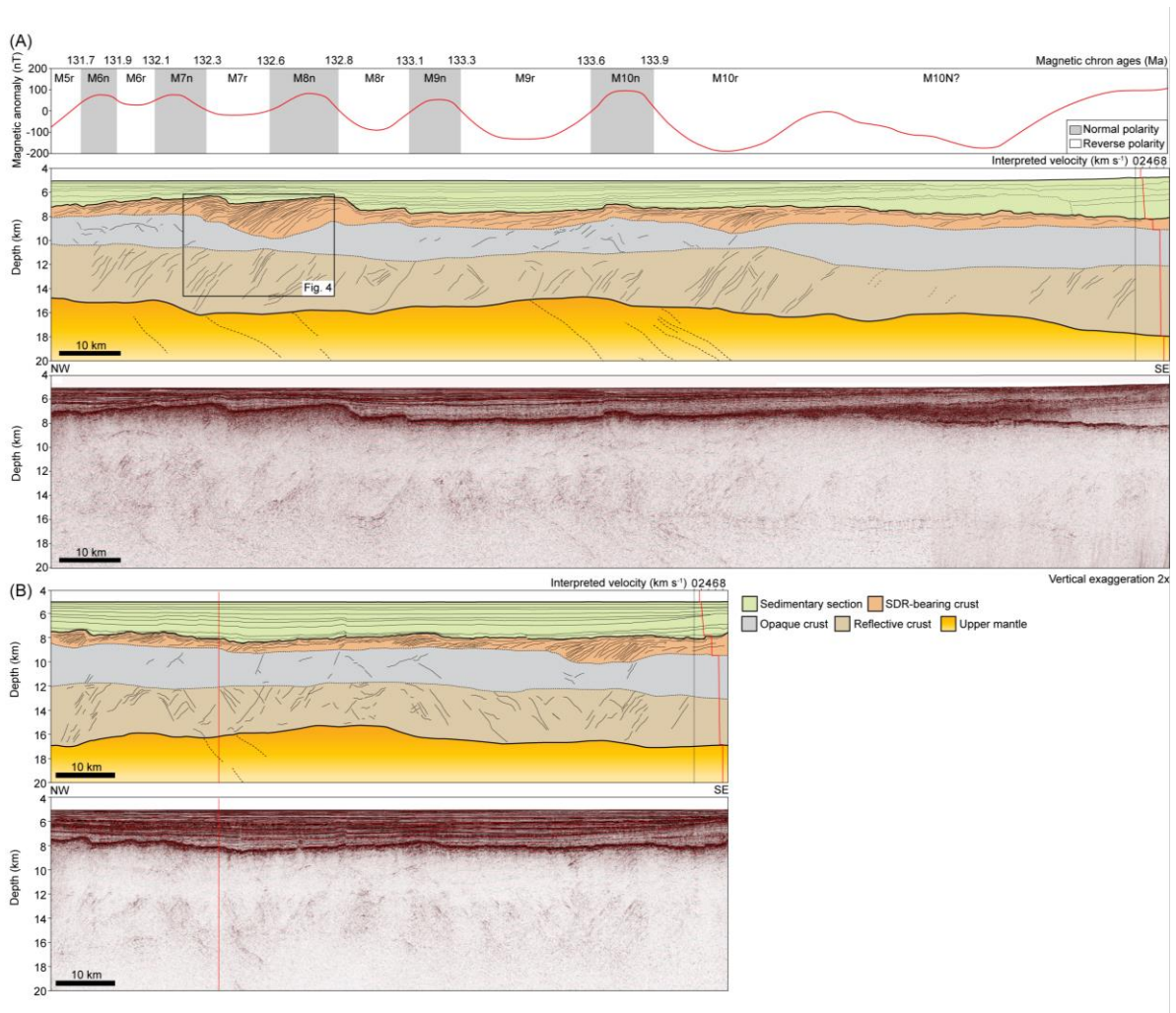
276 **5. Observations and interpretation of the Cuvier Margin structure**

277 5.1. Reflection seismology

278 *5.1.1. Observations*

279 The geological structure imaged in line EW0113-6 is very similar to that of EW0113-5 (Fig.
280 4), supporting the use of velocities from EW0113-6 in depth conversion. A prominent,
281 continuous, high-amplitude seismic reflection is recognised across the CAP and interpreted
282 as the interface between crystalline crust and overlying sedimentary rocks (Fig. 4). The Moho
283 was picked at the base of a flat-lying zone of moderate to high amplitude, discontinuous
284 seismic reflections, and is ~ 17 km deep in the SE, shallowing oceanward on EW0113-5 to
285 ≤ 14 km (Fig. 4A). On EW0113-6, the Moho remains relatively flat at depths of ~ 16 – 17 km
286 (Fig. 4B). Overall, the crystalline crust is ~ 8 – 10 km thick (Fig. 4).

287



288

289

290 Figure 4: Interpreted and uninterpreted, depth-converted seismic lines (A) EW0113-5 and (B)

291 EW0113-6 showing crustal structure of the Cuvier margin. A co-located magnetic anomaly

292 profile showing interpreted magnetic chrons is presented for (A) (after Robb et al., 2005).

293 Seismic data are displayed with reverse polarity, where a downward increase in acoustic

294 impedance is represented by a negative (red) reflection event and a downward decrease in

295 acoustic impedance is a positive (black) reflection event. For details of the velocity model

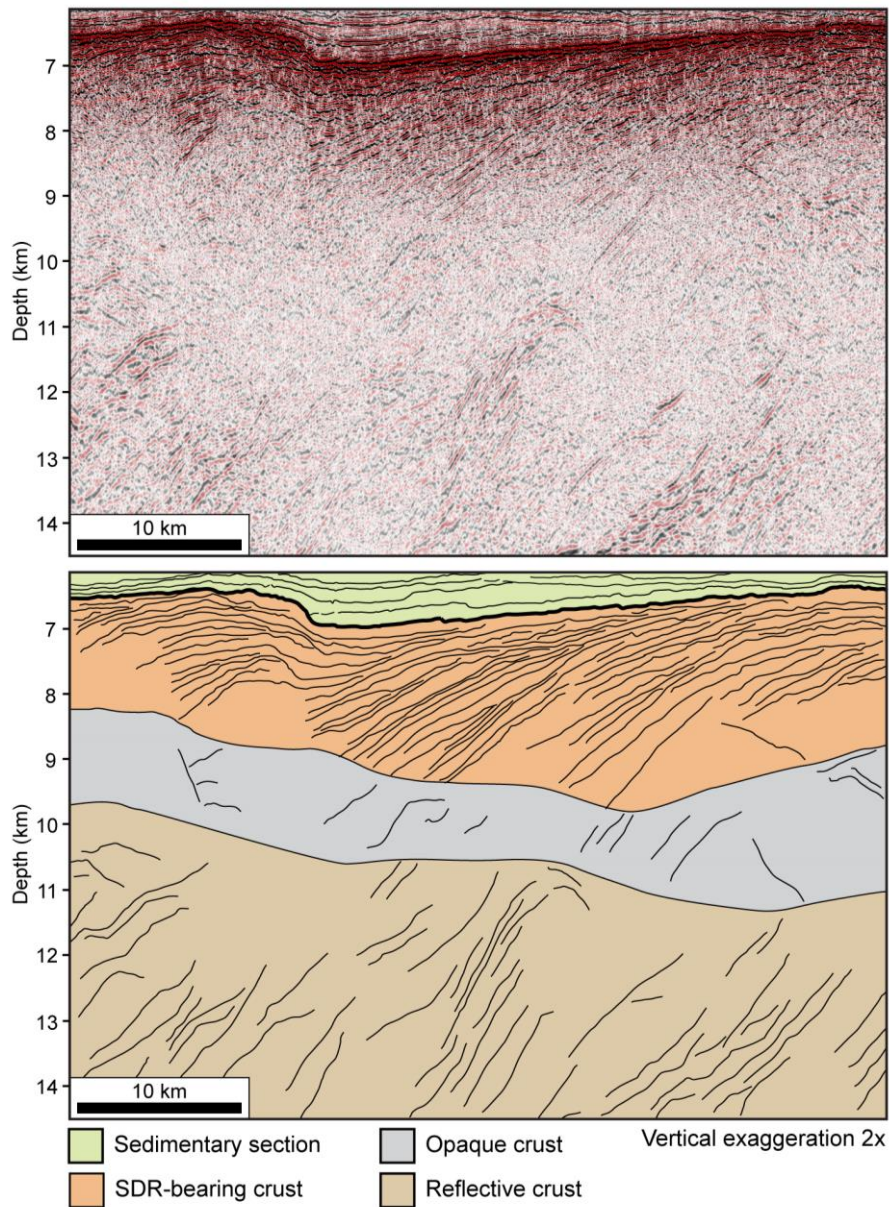
296 used, see supplemental information.

297

298 The 1–3 km-thick, uppermost crystalline crustal layer comprises a layered, moderate-

299 to high-amplitude seismic facies, which locally contains ≤ 20 km wide, ≤ 3 km thick wedges

300 of coherent, high-amplitude, seaward-diverging reflections (Figs 4 and 5). Where well-
301 developed wedges are absent, this crustal layer contains discontinuous, horizontal to gently
302 seaward-dipping reflections (Fig. 4). Seismic velocities for this layer are 4–5 km/s (Fig. 4;
303 Tischer, 2006).
304



305
306 Figure 5: Zoomed in view of EW0113-5 highlighting the seismic character of interpreted
307 SDR packages (see Fig. 4A for location).
308

309 The uppermost crystalline layer is underlain by a low-amplitude, weakly-reflective,
310 1–2.8 km thick, seismic facies layer (i.e. ‘opaque crust’, Figs 4 and 5) and a deeper, low-
311 amplitude, 3.5–6 km-thick, seismic facies layer that locally contains prominent, high-
312 amplitude, dipping reflections (i.e. ‘reflective crust’, Figs 4 and 5). The few reflections that
313 are observed within the opaque crust typically have moderate- to high amplitudes, although
314 low-amplitude also occur, and have variable dips (Figs 4 and 5). Dipping reflections within
315 the reflective crust terminate at the Moho and primarily dip oceanward at 20–30°, although
316 several reflections, particularly on EW0113-6, dip landwards (Figs 4 and 5). Seismic
317 velocities of the opaque and reflective layers are 6.8–7.2 km/s (Fig. 4; Tischer, 2006).

318

319 *5.1.2. Interpretation of crustal structure*

320 Based on their geometry and seismic velocity, we interpret the divergent reflection wedges in
321 the uppermost crystalline crust layer as SDRs, likely comprising interbedded subaerial
322 igneous rocks deposited in lava flows and terrestrial sedimentary strata (Figs 4 and 5) (e.g.,
323 McDermott et al., 2018; Menzies et al., 2002; Planke & Eldholm, 1994). We infer flatter-
324 lying reflections are gently-dipping lavas. The observed structure and velocities of the opaque
325 and reflective crust, defined by transparent seismic facies and discordant high-amplitude
326 reflections respectively (Figs 3 and 4), is consistent with the seismic character of sheeted
327 dyke and lower crustal gabbro intrusions in oceanic crust (e.g., Eittreim et al., 1994; Paton et
328 al., 2017). However, the likelihood that SDR emplacement occurred sub-aerially suggests the
329 CAP could instead comprise COTZ crust. In both the oceanic and COTZ crust scenarios,
330 observed moderate- to high-amplitude reflections within these crustal packages may be
331 interpreted as igneous intrusion contacts, primary layering within gabbros, or lower crustal
332 strain markers (e.g., shear zones) (e.g., Abdelmalak et al., 2015; Paton et al., 2017; Phipps-
333 Morgan & Chen, 1993).

334

335 5.2. Magnetic anomalies

336 Assessment of the EMAG2v2 and ship-track magnetic data reveal 10 km wide, continuous
337 magnetic stripes with lengths of ≤ 220 km across much of the CAP (Figs 1, 3, and 4).

338 Although magnetic anomalies in the EMAG2v3 grid are suppressed relative to EMAG2v2,
339 linear anomalies can still be distinguished across the CAP and in the Gallah Province (Fig. 3).

340 Due to the lower resolution of magnetic anomalies in the EMAG2v3 grid, magnetic chrons
341 cannot be confidently attributed and we thus rely on EMAG2v2 and shiptrack data to define

342 probable chrons (Fig. 3). Proximal to the Australian continent, long-wavelength magnetic
343 anomalies can only be broadly assigned to chron M10N (Figs 1, 3, and 4) (Robb et al., 2005);

344 within the distal 100 km of seismic line EW0113-5, chrons M10n–M5r (~ 135.3 – 131.4 Ma)

345 are clearly defined and have amplitudes of $\leq \pm 100$ nT (Figs 1, 3, and 4). Chrons M8r–M7n

346 coincide with a prominent ≤ 3 km thick, ~ 25 km long, package of seaward-dipping reflectors
347 in the uppermost crystalline crust layer (Fig. 4A).

348 Robb et al. (2005) interpret the magnetic anomalies M10N–M6 southeast of the

349 Sonne Ridge as conjugate to a more poorly developed set of anomalies northwest of the ridge
350 (Fig. 1). These poorly defined chrons (i.e. M10N–M6) northwest of the Sonne Ridge

351 terminate abruptly against the Cape Range Fracture Zone, abutting younger magnetic chrons

352 on the Gascoyne Abyssal Plain (Fig. 1). Chron M5n is the first to occur continuously along-

353 strike across both the Cuvier and Gascoyne margin segments (Fig. 1).

354

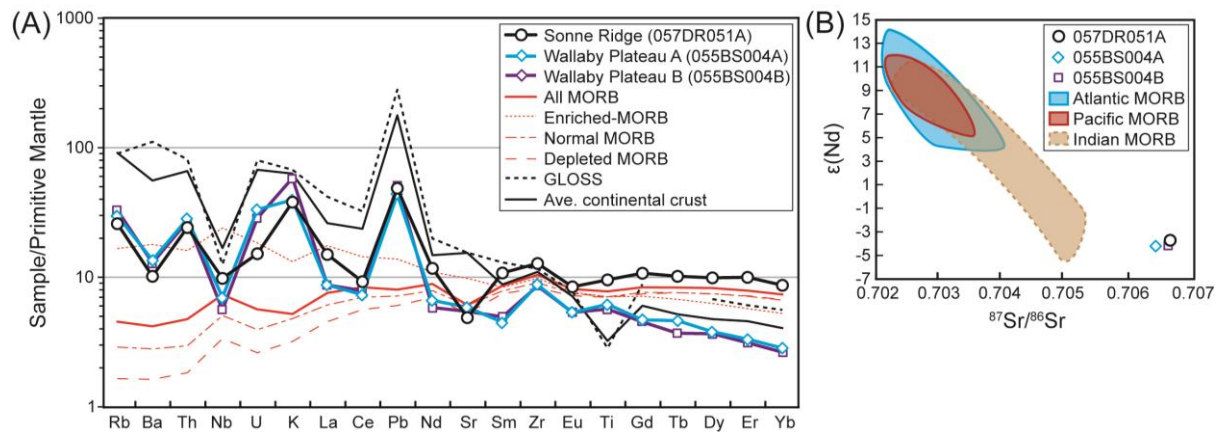
355 5.3. Geochemistry of basalts dredged from the Sonne Ridge

356 The only basalt collected from the Sonne Ridge displays a relatively flat, Rare Earth Element

357 (REE) pattern (Fig. 6A). Based on this observation, Dadd et al. (2015) interpret the basalt to

358 have a slightly enriched MORB-like source, supporting the inference that the CAP comprises

359 oceanic crust (e.g., Hopper et al., 1992; Larson et al., 1979; Mihut & Müller, 1998). Although
360 a flat REE pattern can be indicative of the shallow melting regime of MORB generation, it
361 does not preclude other settings. By replotting the trace element and radiogenic isotopic
362 compositions of the Sonne Ridge sample, we show the sample has characteristics that could
363 be suggestive of a more continental source (Fig. 5). It must be kept in mind that the Sonne
364 Ridge sample is heavily altered (Dadd et al., 2015), which likely explains the elemental
365 enrichment in Pb, Ba, and Rb, as well as elevated $^{87}\text{Sr}/^{86}\text{Sr}$. However, the negative Nb
366 anomaly, in part defined by neighbouring element Th that is unlikely to be affected by
367 contamination, and unradiogenic ϵ_{Nd} , cannot be ascribed to alteration (Fig. 6). Instead, the
368 negative Nb anomaly and unradiogenic ϵ_{Nd} can be interpreted as a chemically evolved,
369 continental or sedimentary contribution to the magmas. Finally, the chemical similarity of the
370 Sonne Ridge basalt to two ~124 Ma samples from the Wallaby Plateau (Fig. 6) is notable
371 because this area is interpreted to comprise intruded continental crust, supported by the
372 recovery of pre-breakup sedimentary rocks from the plateau during dredging (Daniell et al.,
373 2009; Olierook et al., 2015; Stilwell et al., 2012). Therefore, the chemical characteristics of
374 the Sonne Ridge lava suggest the basalt could originate from either melting of sub-
375 continental lithospheric mantle (SCLM) or contamination of a MORB-like magma by
376 assimilation as it ascended through continental crust (cf. Dadd et al., 2015). Importantly, the
377 Sonne Ridge likely represents the rift/spreading axis of the CAP (Robb et al., 2005), such that
378 the basalt sample represents one of the youngest magmas within the system. We thus
379 consider it plausible that older magmas emanating from the ridge system, including the SDRs
380 imaged in the seismic reflection data, could have a more pronounced continental signature.
381



382

383

384 Figure 6: (A) Primitive mantle normalized incompatible element diagram comparing the
 385 dredged Sonne Ridge and Wallaby Plateau basalt lava samples with average (ave.)
 386 compositions of MORB variants (Hofmann, 2014), Globally Subducting Sediment (GLOSS)
 387 (Plank & Langmuir, 1998), and continental crust (Rudnick & Fountain, 1995). (B) Plot of
 388 $\epsilon(\text{Nd})$ versus $^{87}\text{Sr}/^{86}\text{Sr}$, illustrating that the Sonne Ridge and Wallaby Plateau samples are
 389 distinct from MORB (based on data collated in Hofmann, 2014).

390

391 6. Discussion

392 6.1. Nature of the Cuvier margin crust

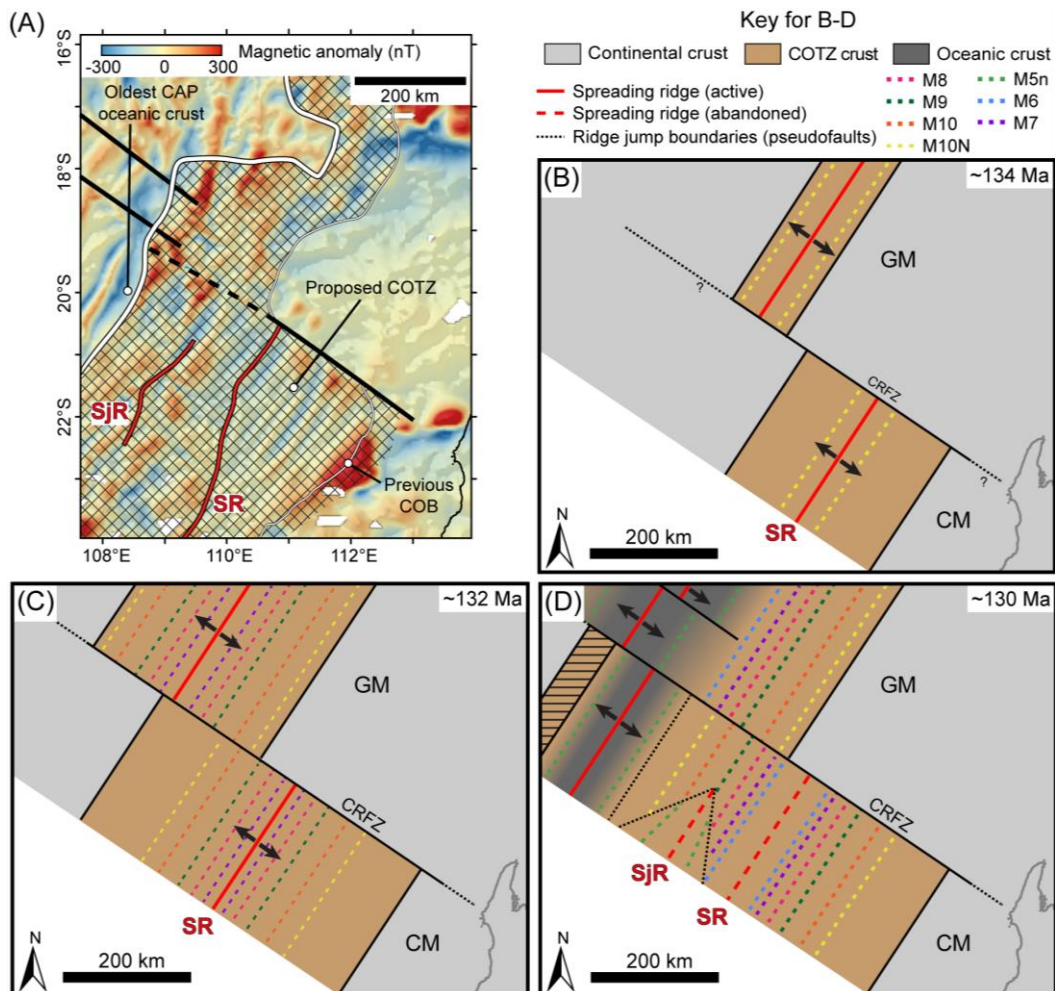
393 Subsidence profiles for normal oceanic crust predict mid-ocean ridge axes at water depths of
 394 ~ 3 km and subsidence rates of ~ 90 m/Myr for the first 10 Ma after break-up (e.g., Menard,
 395 1969; Parsons & Sclater, 1977; Stein & Stein, 1992). We identify a previously unrecognised
 396 upper-crustal crystalline basement layer within the CAP that contains well-developed, ≤ 3
 397 km-thick, SDRs and extends >200 km seaward from the previously-interpreted COTZ (Figs
 398 1, 4, and 5). Packages of SDRs observed and drilled on other continental margins indicate the
 399 comprising lavas extruded sub-aerially and are typically overlain by sub-aerial to shallow-
 400 marine strata deposited during subsequent margin subsidence (e.g., Larsen et al., 1994).

401 Although the observed SDRs across the CAP are not drilled, linking their origin to sub-aerial

402 volcanism conforms with observations from DSDP site 263 (Fig. 1), which intersected Early
403 Cretaceous (≤ 130.8 Ma), shallow-marine sedimentary rocks immediately deposited
404 immediately on top of the crystalline basement (Veevers & Johnstone, 1974; Willcox &
405 Exon, 1976). The presence of SDRs and overlying shallow-marine sedimentary rocks
406 suggests sub-aerial to shallow-marine conditions were prevalent across the Cuvier margin
407 during formation of the CAP, which is inconsistent with subsidence profiles for normal
408 oceanic crust (e.g., Menard, 1969; Parsons & Sclater, 1977; Stein & Stein, 1992). One
409 possible explanation for the observed sub-aerial to shallow-marine conditions is that the CAP
410 actually comprises COTZ crust rather than oceanic crust, having formed through sub-aerial
411 rifting and spreading (Fig. 7D) (cf. Collier et al., 2017; McDermott et al., 2018; Paton et al.,
412 2017). The chemistry of a basalt sample from the Sonne Ridge, particularly its Nd isotopic
413 composition and refractory trace element abundances (Fig. 6), allows for a contribution of
414 sub-continental lithospheric mantle (SCLM) or interaction with continental crust, supporting
415 the hypothesis that full continental rupture may not have occurred even during the final
416 phases of CAP spreading.

417 We interpret the previously recognised SDRs beneath the continental slope on the
418 Cuvier margin (Hopper et al., 1992; Symonds et al., 1998) as marking the transition from
419 mechanical- to magma-dominated rifting and the landward limit of the COTZ, which likely
420 comprises heavily intruded continental crust (i.e. ‘transitional’ crust) (Fig. 7A). A progressive
421 localisation in dyking as rifting continued led to the eventual generation of the sub-aerial
422 Sonne Ridge, which was perhaps akin to 20 km wide Quaternary magmatic segments in the
423 Ethiopian Rift (e.g., Ebinger & Casey, 2001; Hayward & Ebinger, 1996; Kendall et al.,
424 2005), where the crust likely comprises $>50\%$ new mafic material (Daniels et al., 2014). Our
425 proposed crustal structure for the CAP therefore involves a gradual north-westwards change
426 from continental crust into COTZ crust, which we suggest is likely characterised by

427 ‘transitional’ crust in the SE and becomes increasingly ‘magmatic’ towards the Sonne Ridge
 428 (Figs 2 and 7). This gradual change in style of the COTZ is consistent with progression from
 429 Type I to Type II SDR sequences, which are located above transitional and magmatic crust
 430 respectively, observed offshore S America (McDermott et al., 2018). It is plausible remnants
 431 of thinned continental blocks may have been incorporated into the COTZ crust during rift
 432 jumps (Gibbons et al., 2012; Robb et al., 2005). Importantly, our model implies the Sonne
 433 Ridge is not an extinct submarine, oceanic spreading centre (e.g., Falvey & Veevers, 1974;
 434 Larson et al., 1979; MacLeod et al., 2017; Mihut & Müller, 1998; Robb et al., 2005)
 435



436

437

438 Figure 7: (A) Map showing the potential limits of the COTZ based on interpreting the Cap
439 and Gallah Province as transitional and/or magmatic crust. (B-D) Schematic maps showing
440 the development of COTZ crust and the onset of oceanic crust accretion adjacent to the
441 Gascoyne and Cuvier margins, during formation of chrons (B) M10, (C) M6 and (D) M3r.
442 See Figure 1 for chron ages. Location of present day coastline shown for reference.

443

444 Linear magnetic stripes recorded across the CAP reveal an apparent conjugate set of
445 chrons M10N–M6 centred on the Sonne Ridge (Robb et al., 2005), suggesting our inferred
446 COTZ crust may extend out to chron M5n, broadly coincident with the north-western limit of
447 the Gallah Province on the Gascoyne margin (Figs 1 and 7B). Magnetic reversals in the
448 Gallah Province are similar, albeit less developed, to those in the CAP (Direen et al., 2008;
449 Robb et al., 2005). Direen et al. (2008) argue these magnetic anomalies resulted from the
450 stacking of wedges of positively magnetised basalts (including SDRs) and variably
451 magnetised volcanoclastic conglomerates atop transitional magmatic and modified continental
452 crust. We thus suggest that magnetic anomalies along the Gascoyne margin sector are also
453 likely related to geomagnetic polarity reversals recorded by COTZ crust underlying the
454 SDRs. Chemical signatures indicating continental lithosphere contamination, similar to those
455 identified in the CAP, are recorded in basalts from the Gascoyne margin (Direen et al., 2008).

456

457 *6.1.1. Tectonic-magmatic evolution of the Cuvier and Gascoyne margins*

458 During chrons M10N–M5r (i.e. ~136–131 Ma), we suggest stretching and intrusion of
459 continental crust adjacent to both the Gascoyne and Cuvier margins produced COTZ crust,
460 likely comprising transitional crust, which evolved into magmatic crust as intrusion became
461 localised and the proportion of remnant continental crust decreased (Figs 7B–D). Robb et al.
462 (2005) proposed that, during chron M5r–M5n (~131 Ma), a ridge jump in the Cuvier sector

463 led to abandonment of the Sonne Ridge, with a short-lived period of spreading about the
464 Sonja Ridge preceding development of a new ridge ~250 km northwest of the Sonne Ridge
465 (Fig. 7D). We consider that this jump linked the Cuvier and Gascoyne ridges, promoting the
466 onset of true seafloor spreading from chron M3r (~130 Ma) onwards in both sectors (Fig.
467 7D). This initiation of oceanic crust formation transferred the conjugate region of COTZ
468 crust recording M10N-M6 anomalies to the Australian plate (Fig. 7D). With the recognition
469 of a >500 km wide zone of COTZ crust, our interpretation implies that the outer limit of NW
470 Australia's COTZ in the Cuvier margin sector may be positioned substantially further
471 oceanward (>500 km) than previously interpreted (Fig. 7A). Extension of the COTZ across
472 the CAP has implications for the timing and kinematics of plate reconstructions of the NW
473 Australian margin, with the onset of true seafloor spreading potentially ~3 Myr later than
474 suggested by previous studies (e.g., Robb et al., 2005).

475

476 **6.2. Development of magnetic stripes during breakup**

477 Stacked SDR wedges on the CAP overlie COTZ crust and span several chrons (e.g. M8n-
478 M7r, Fig. 3), indicating the magnetic stripes likely record magnetic reversal signatures
479 originating from sub-SDR rocks. Recent forward magnetic modelling of conjugate, ship-track
480 magnetic profiles by Collier et al. (2017) suggest magnetic signals over SDRs arise from a
481 combination of stacked and rotated lavas, producing a long-wavelength positive anomaly that
482 can sometimes mask reversals, and linear magnetic anomalies caused by dyke intrusion in the
483 underlying crust. This is consistent with studies of onshore incipient spreading centres (e.g.
484 Ethiopia), where magnetic anomalies likely originate from axial intrusion by dykes in heavily
485 intruded upper continental crust (Bridges et al., 2012). We suggest that the well-developed
486 linear anomalies over the CAP may therefore originate from intrusions in the COTZ crust
487 underlying the SDRs.

488 The lack of broad positive magnetic anomalies over the transitional to magmatic crust
489 of the CAP may be due to the relatively low SDR thickness (≤ 3 km) compared to the South
490 Atlantic margins (< 8 km thick; Collier et al., 2017). The less-clearly developed and higher
491 amplitude magnetic reversals on the Gascoyne Abyssal Plain may relate to interference from
492 the greater SDR thicknesses (≤ 5.5 km) relative to the Cuvier margin (Direen et al., 2008). We
493 suggest that SDR thickness and, thereby, preservation of magnetic anomalies within
494 transitional or magmatic crust can partly be attributed to extension rate. For example, the
495 extension rate during SDR eruption offshore NW Australia (~ 4.5 cm/yr half rate; Robb et al.,
496 2005) is substantially faster than the inferred extension rates for the South Atlantic during
497 magmatic crust formation (~ 1.1 cm/yr half-rate; Paton et al., 2017). Slower extension rates
498 (e.g. South Atlantic) likely promote stacking of lava flows (Eagles et al., 2015), leading to
499 interference and development of the long-wavelength positive magnetic anomalies (e.g.,
500 Moulin et al., 2010). Extension rate may also influence magnetic anomaly development by
501 affecting the width of magnetic stripes: reversal anomalies will be narrowest at slow
502 spreading ridges (Vine, 1966). The narrower anomalies, combined with the greater potential
503 for vertical stacking of lavas, will tend to suppress magnetic anomaly preservation.

504

505 **6. Conclusions**

506 We present evidence for a previously unrecognised, > 500 km-wide region of continent-ocean
507 transition zone (COTZ) crust adjacent to the Northwest Australian continental margin. We
508 suggest the COTZ crust likely comprises a spectrum of ‘transitional’, i.e. heavily intruded
509 continental crust, and ‘magmatic’ crust formed by addition of igneous material at a sub-aerial
510 ridge. This COTZ crust records well-developed linear magnetic reversal anomalies. Seaward-
511 dipping reflectors (SDRs) overlie the 5–8.5 km thick COTZ crust, which hosts intrusions that
512 are the primary source of the observed magnetic signal. The recognition of this region of

513 COTZ crust implies that the outer limit of Australia's continent-ocean transition zone may be
514 >500 km further oceanward than previously interpreted. That COTZ crust on volcanic
515 margins can record the development of clear seafloor spreading-type magnetic stripes,
516 implies magnetic stripes alone are not a reliable proxy for the onset of seafloor spreading and
517 the extent of oceanic crust.

518

519 **7. Acknowledgements**

520 Schlumberger are thanked for provision of Petrel software licenses. M.T.R. was supported by
521 NERC grant NE/L501621/L. The EW0113 seismic survey and EMAG2 magnetic anomaly
522 grids were, and can be acquired from, the UTIG Marine Geoscience Data System and the
523 NOAA National Geophysical Data Centre, respectively. Gwenn Peron-Pinvidic, Gareth
524 Roberts, and Saskia Goes are thanked for helpful discussions during the preparation of this
525 manuscript. We thank three reviewers for their constructive comments on a previous version
526 of this manuscript.

527

528 **Figure Captions**

529 Figure 1: (A) Location map of the study area highlighting key tectonic elements, including
530 areas of recognised seaward-dipping reflectors (SDRs) (Holford et al., 2013; Symonds et al.,
531 1998) and previously interpreted approximate (approx.) limits of the continent-ocean
532 boundary (COB; Eagles et al., 2015) and continent-ocean transition zones (COTZs; Direen et
533 al., 2008; Symonds et al., 1998). Inset: study area location offshore NW Australia. AAP –
534 Argo Abyssal Plain, CAP – Cuvier Abyssal Plain, CRFZ – Cape Range Fracture Zone, GAP
535 – Gascoyne Abyssal Plain, GP – Gallah Province, NCB – North Carnarvon Basin, SCB –
536 South Carnarvon Basin, Cu – Cuvier margin COTZ, SR – Sonne Ridge, Sjr – Sonja Ridge,
537 WP – Wallaby Plateau, WS – Wallaby Saddle, WZFZ – Wallaby-Zenith Fracture Zone.

538 Dredge sites 55 (samples 055BS004A and 055BS004B) and 57 (sample 057DR051A) are
539 also shown (Dadd et al., 2015). (B) Total magnetic intensity grid (EMAG2v2), interpreted
540 magnetic chrons (based on Robb et al., 2005). See Supplementary Figure S1 for an
541 uninterpreted version.

542

543 Figure 2: Schematic model (not to scale) of a continent-ocean transition zone along a
544 volcanic passive margin; for simplicity the lithospheric mantle is not shown. As magma
545 intrudes continental crust, likely as dykes at mid- to upper-crustal levels and larger gabbroic
546 bodies in the lower crust, it becomes ‘transitional crust’ (e.g., Eldholm et al., 1989).
547 Continued intrusion and dyking leads to localisation of magmatism within narrow zones
548 where sub-aerial spreading dominates extension and there is little, if any, continental crust
549 remaining (i.e. magmatic crust) (i.e. ‘magmatic crust’; e.g., Collier et al., 2017; Paton et al.,
550 2017). We categorize transitional and magmatic crust as ‘COTZ crust’. Sub-aerial spreading
551 centres may feed extensive lava flows that later, through subsidence, become seaward-
552 dipping reflectors (SDRs); SDR subsidence leads to rotation of underlying dykes
553 (Abdelmalak et al., 2015). A similar rotation of lavas and dykes is observed in oceanic crust
554 (Karson, 2019).

555

556 Figure 3: Total magnetic intensity grids EMAG2v2 and EMAG2v3 (Maus et al., 2009; Meyer
557 et al., 2017), compared with shiptrack magnetic data (Robb et al., 2005). Key tectonic
558 elements also shown (see Fig. 1 for legend).

559

560 Figure 4: Interpreted and uninterpreted, depth-converted seismic lines (A) EW0113-5 and (B)
561 EW0113-6 showing crustal structure of the Cuvier margin. A co-located magnetic anomaly
562 profile showing interpreted magnetic chrons is presented for (A) (after Robb et al., 2005).

563 Seismic data are displayed with reverse polarity, where a downward increase in acoustic
564 impedance is represented by a negative (red) reflection event and a downward decrease in
565 acoustic impedance is a positive (black) reflection event. For details of the velocity model
566 used, see supplemental information.

567

568 Figure 5: Zoomed in view of EW0113-5 highlighting the seismic character of interpreted
569 SDR packages (see Fig. 4A for location).

570

571 Figure 6: (A) Primitive mantle normalized incompatible element diagram comparing the
572 dredged Sonne Ridge and Wallaby Plateau basalt lava samples with average (ave.)
573 compositions of MORB variants (Hofmann, 2014), Globally Subducting Sediment (GLOSS)
574 (Plank & Langmuir, 1998), and continental crust (Rudnick & Fountain, 1995). (B) Plot of
575 $\epsilon(\text{Nd})$ versus $^{87}\text{Sr}/^{86}\text{Sr}$, illustrating that the Sonne Ridge and Wallaby Plateau samples are
576 distinct from MORB (based on data collated in Hofmann, 2014).

577

578 Figure 7: (A) Map showing the potential limits of the COTZ based on interpreting the Cap
579 and Gallah Province as transitional and/or magmatic crust. (B-D) Schematic maps showing
580 the development of COTZ crust and the onset of oceanic crust accretion adjacent to the
581 Gascoyne and Cuvier margins, during formation of chrons (B) M10, (C) M6 and (D) M3r.
582 See Figure 1 for chron ages. Location of present day coastline shown for reference.

583

584 **References**

585 Abdelmalak, M. M., Andersen, T. B., Planke, S., Faleide, J. I., Corfu, F., Tegner, C., et al.
586 (2015). The ocean-continent transition in the mid-Norwegian margin: Insight from
587 seismic data and an onshore Caledonian field analogue. *Geology*, 43(11), 1011-1014.
588 Bridges, D. L., Mickus, K., Gao, S. S., Abdelsalam, M. G., & Alemu, A. (2012). Magnetic
589 stripes of a transitional continental rift in Afar. *Geology*, 40(3), 203-206.

- 590 Bronner, A., Sauter, D., Manatschal, G., Péron-Pinvidic, G., & Munschy, M. (2011).
591 Magmatic breakup as an explanation for magnetic anomalies at magma-poor rifted
592 margins. *Nature Geoscience*, 4(8), 549.
- 593 Collier, J. S., McDermott, C., Warner, G., Gyori, N., Schnabel, M., McDermott, K., & Horn,
594 B. W. (2017). New constraints on the age and style of continental breakup in the
595 South Atlantic from magnetic anomaly data. *Earth and Planetary Science Letters*,
596 477, 27-40.
- 597 Colwell, J., Symonds, P., & Crawford, A. (1994). The nature of the Wallaby (Cuvier) Plateau
598 and other igneous provinces of the west Australian margin. *Journal of Australian
599 Geology and Geophysics*, 15, 137-156.
- 600 Crawford, A. J., & von Rad, U. (1994). The petrology, geochemistry and implications of
601 basalts dredged from the Rowley Terrace-Scott Plateau and Exmouth Plateau
602 margins, northwestern Australia. *Journal of Australian Geology and Geophysics*, 15,
603 43-54.
- 604 Dadd, K. A., Kellerson, L., Borissova, I., & Nelson, G. (2015). Multiple sources for volcanic
605 rocks dredged from the Western Australian rifted margin. *Marine Geology*, 368, 42-
606 57.
- 607 Daniell, J., Jorgensen, D., Anderson, T., Borissova, I., Burq, S., Heap, A., et al. (2009).
608 Frontier basins of the West Australian continental margin. *Geoscience Australia
609 Record*, 38, 243.
- 610 Daniels, K. A., Bastow, I. D., Keir, D., Sparks, R. S. J., & Menand, T. (2014). Thermal
611 models of dyke intrusion during development of continent–ocean transition. *Earth
612 and Planetary Science Letters*, 385(0), 145-153.
- 613 Direen, N. G., Stagg, H. M. J., Symonds, P. A., & Colwell, J. B. (2008). Architecture of
614 volcanic rifted margins: new insights from the Exmouth – Gascoyne margin, Western
615 Australia. *Australian Journal of Earth Sciences*, 55(3), 341-363.
- 616 Eagles, G., Pérez-Díaz, L., & Scarselli, N. (2015). Getting over continent ocean boundaries.
617 *Earth-Science Reviews*, 151, 244-265.
- 618 Ebinger, C. J., & Casey, M. (2001). Continental breakup in magmatic provinces: An
619 Ethiopian example. *Geology*, 29(6), 527.
- 620 Eittreim, S. L., Gribidenko, H., Helsley, C. E., Sliter, R., Mann, D., & Ragozin, N. (1994).
621 Oceanic crustal thickness and seismic character along a central Pacific transect.
622 *Journal of Geophysical Research: Solid Earth*, 99(B2), 3139-3145.
- 623 Eldholm, O., Thiede, J., & Taylor, E. (1989). *The Norwegian continental margin: tectonic,
624 volcanic, and paleoenvironmental framework*. Paper presented at the Proceedings of
625 the ocean drilling program, Scientific results.
- 626 Falvey, D., & Veevers, J. (1974). Physiography of the Exmouth and Scott plateaus, western
627 Australia, and adjacent northeast Wharton Basin. *Marine Geology*, 17(2), 21-59.
- 628 Gibbons, A. D., Barckhausen, U., den Bogaard, P., Hoernle, K., Werner, R., Whittaker, J. M.,
629 & Müller, R. D. (2012). Constraining the Jurassic extent of Greater India: Tectonic
630 evolution of the West Australian margin. *Geochemistry, Geophysics, Geosystems*,
631 13(5).
- 632 Gradstein, F., & Ogg, J. (2012). The chronostratigraphic scale. In *The geologic time scale*
633 (pp. 31-42): Elsevier.
- 634 Hayward, N., & Ebinger, C. (1996). Variations in the along-axis segmentation of the Afar
635 Rift system. *Tectonics*, 15(2), 244-257.
- 636 Heine, C., & Müller, R. (2005). Late Jurassic rifting along the Australian North West Shelf:
637 margin geometry and spreading ridge configuration. *Australian Journal of Earth
638 Sciences*, 52(1), 27-39.

- 639 Hey, R. (1977). A new class of “pseudofaults” and their bearing on plate tectonics: A
640 propagating rift model. *Earth and Planetary Science Letters*, 37(2), 321-325.
- 641 Hofmann, A. (2014). Sampling mantle heterogeneity through oceanic basalts: Isotopes and
642 trace elements. In C. RW (Ed.), *The Mantle and Core, Treatise on Geochemistry* (pp.
643 67-101). Oxford: Elsevier-Pergamon.
- 644 Holford, S. P., Schofield, N., Jackson, C. A. L., Magee, C., Green, P. F., & Duddy, I. R.
645 (2013). Impacts of igneous intrusions on source and reservoir potential in prospective
646 sedimentary basins along the western Australian continental margin. In M. Keep & S.
647 J. Moss (Eds.), *The Sedimentary Basins of Western Australia IV*. Perth, WA:
648 Proceedings of the Petroleum Exploration Society of Australia Symposium.
- 649 Hopper, J. R., Mutter, J. C., Larson, R. L., & Mutter, C. Z. (1992). Magmatism and rift
650 margin evolution: Evidence from northwest Australia. *Geology*, 20(9), 853-857.
- 651 Karson, J. A. (2019). From Ophiolites to Oceanic Crust: Sheeted Dike Complexes and
652 Seafloor Spreading. In R. Srivastava, R. Ernst, & P. Peng (Eds.), *Dyke Swarms of the*
653 *World: A Modern Perspective* (pp. 459-492): Springer.
- 654 Kendall, J.-M., Stuart, G., Ebinger, C., Bastow, I., & Keir, D. (2005). Magma-assisted rifting
655 in Ethiopia. *Nature*, 433(7022), 146-148.
- 656 Keranen, K., Klemperer, S., Gloaguen, R., & Group, E. W. (2004). Three-dimensional
657 seismic imaging of a protoridge axis in the Main Ethiopian rift. *Geology*, 32(11), 949-
658 952.
- 659 Larsen, H., & Saunders, A. (1998). *41. Tectonism and volcanism at the Southeast Greenland*
660 *rifted margin: a record of plume impact and later continental rupture*. Paper
661 presented at the Proceedings of the Ocean Drilling Program, Scientific Results.
- 662 Larsen, H., Saunders, A., Larsen, L., & Lykke-Andersen, H. (1994). ODP activities on the
663 South-East Greenland margin: Leg 152 drilling and continued site surveying. *Rapport*
664 *Grønlands Geologiske Undersøgelse*, 160, 75-81.
- 665 Larson, R. L., Mutter, J. C., Diebold, J. B., Carpenter, G. B., & Symonds, P. (1979). Cuvier
666 Basin: a product of ocean crust formation by Early Cretaceous rifting off Western
667 Australia. *Earth and Planetary Science Letters*, 45(1), 105-114.
- 668 Longley, I., Buessenschuett, C., Clydsdale, L., Cubitt, C., Davis, R., Johnson, M., et al.
669 (2002). The North West Shelf of Australia—a Woodside perspective. *The sedimentary*
670 *basins of Western Australia*, 3, 27-88.
- 671 Mackenzie, G., Thybo, H., & Maguire, P. (2005). Crustal velocity structure across the Main
672 Ethiopian Rift: results from two-dimensional wide-angle seismic modelling.
673 *Geophysical Journal International*, 162(3), 994-1006.
- 674 MacLeod, S. J., Williams, S. E., Matthews, K. J., Müller, R. D., & Qin, X. (2017). A global
675 review and digital database of large-scale extinct spreading centers. *Geosphere*, 13(3),
676 911-949.
- 677 Maguire, P., Keller, G., Klemperer, S., Mackenzie, G., Keranen, K., Harder, S., et al. (2006).
678 Crustal structure of the northern Main Ethiopian Rift from the EAGLE controlled-
679 source survey; a snapshot of incipient lithospheric break-up. *SPECIAL*
680 *PUBLICATION-GEOLOGICAL SOCIETY OF LONDON*, 259, 269.
- 681 Maus, S., Barckhausen, U., Berkenbosch, H., Bournas, N., Brozena, J., Childers, V., et al.
682 (2009). EMAG2: A 2-arc min resolution Earth Magnetic Anomaly Grid compiled
683 from satellite, airborne, and marine magnetic measurements. *Geochemistry*,
684 *Geophysics, Geosystems*, 10(8).
- 685 McDermott, C., Lonergan, L., Collier, J. S., McDermott, K. G., & Bellingham, P. (2018).
686 Characterization of Seaward-Dipping Reflectors Along the South American Atlantic
687 Margin and Implications for Continental Breakup. *Tectonics*, 37(9), 3303-3327.

- 688 Menard, H. (1969). Elevation and subsidence of oceanic crust. *Earth and Planetary Science*
689 *Letters*, 6(4), 275-284.
- 690 Menzies, M., Klemperer, S., Ebinger, C., & Baker, J. (2002). Characteristics of volcanic
691 rifted margins. In M. Menzies, S. Klemperer, C. Ebinger, & J. Baker (Eds.), *Volcanic*
692 *Rifted Margins, Special Publications* (Vol. 362, pp. 1-14): Geological Society of
693 America.
- 694 Meyer, B., Chulliat, A., & Saltus, R. (2017). Derivation and error analysis of the Earth
695 Magnetic Anomaly Grid at 2 arc min Resolution Version 3 (EMAG2v3).
696 *Geochemistry, Geophysics, Geosystems*, 18(12), 4522-4537.
- 697 Mihut, D., & Müller, R. D. (1998). Volcanic margin formation and Mesozoic rift propagators
698 in the Cuvier Abyssal Plain off Western Australia. *Journal of Geophysical Research*,
699 103(B11), 27135-27127,27149.
- 700 Moulin, M., Aslanian, D., & Unternehr, P. (2010). A new starting point for the South and
701 Equatorial Atlantic Ocean. *Earth-Science Reviews*, 98(1-2), 1-37.
- 702 Olierook, H. K., Merle, R. E., Jourdan, F., Sircombe, K., Fraser, G., Timms, N. E., et al.
703 (2015). Age and geochemistry of magmatism on the oceanic Wallaby Plateau and
704 implications for the opening of the Indian Ocean. *Geology*, 43(11), 971-974.
- 705 Parsons, B., & Sclater, J. G. (1977). An analysis of the variation of ocean floor bathymetry
706 and heat flow with age. *Journal of Geophysical Research*, 82(5), 803-827.
- 707 Paton, D., Pindell, J., McDermott, K., Bellingham, P., & Horn, B. (2017). Evolution of
708 seaward-dipping reflectors at the onset of oceanic crust formation at volcanic passive
709 margins: Insights from the South Atlantic. *Geology*, 45(5), 439-442.
- 710 Phipps-Morgan, J., & Chen, Y. J. (1993). The genesis of oceanic crust: Magma injection,
711 hydrothermal circulation, and crustal flow. *Journal of Geophysical Research: Solid*
712 *Earth*, 98(B4), 6283-6297.
- 713 Plank, T., & Langmuir, C. H. (1998). The chemical composition of subducting sediment and
714 its consequences for the crust and mantle. *Chemical Geology*, 145(3), 325-394.
- 715 Planke, S., & Eldholm, O. (1994). Seismic response and construction of seaward dipping
716 wedges of flood basalts: Vøring volcanic margin. *Journal of Geophysical Research:*
717 *Solid Earth*, 99(B5), 9263-9278.
- 718 Rabinowitz, P. D., & LaBrecque, J. (1979). The Mesozoic South Atlantic Ocean and
719 evolution of its continental margins. *Journal of Geophysical Research: Solid Earth*,
720 84(B11), 5973-6002.
- 721 Robb, M. S., Taylor, B., & Goodliffe, A. M. (2005). Re-examination of the magnetic
722 lineations of the Gascoyne and Cuvier Abyssal Plains, off NW Australia. *Geophysical*
723 *Journal International*, 163(1), 42-55.
- 724 Rooney, T. O., Bastow, I. D., Keir, D., Mazzarini, F., Movsesian, E., Grosfils, E. B., et al.
725 (2014). The protracted development of focused magmatic intrusion during continental
726 rifting. *Tectonics*, 33(6), 875-897.
- 727 Rudnick, R. L., & Fountain, D. M. (1995). Nature and composition of the continental crust: a
728 lower crustal perspective. *Reviews of Geophysics*, 33(3), 267-309.
- 729 Stagg, H., Alcock, M., Bernardel, G., Moore, A., Symonds, P., & Exon, N. (2004).
730 *Geological framework of the outer Exmouth Plateau and adjacent ocean basins:*
731 Geoscience Australia.
- 732 Stein, C. A., & Stein, S. (1992). A model for the global variation in oceanic depth and heat
733 flow with lithospheric age. *Nature*, 359(6391), 123.
- 734 Stilwell, J., Quilty, P., & Mantle, D. (2012). Paleontology of Early Cretaceous deep-water
735 samples dredged from the Wallaby Plateau: new perspectives of Gondwana break-up
736 along the Western Australian margin. *Australian Journal of Earth Sciences*, 59(1),
737 29-49.

- 738 Symonds, P. A., Planke, S., Frey, O., & Skogseid, J. (1998). Volcanic evolution of the
739 Western Australian Continental Margin and its implications for basin development.
740 *The Sedimentary Basins of Western Australia 2: Proc. of Petroleum Society Australia*
741 *Symposium, Perth, WA.*
- 742 Talwani, M., & Eldholm, O. (1973). Boundary between continental and oceanic crust at the
743 margin of rifted continents. *Nature*, 241(5388), 325.
- 744 Tischer, M. (2006). *The structure and development of the continent-ocean transition zone of*
745 *the Exmouth Plateau and Cuvier margin, Northwest Australia: implications for*
746 *extensional strain partitioning.* (PhD), Columbia University,
- 747 Veevers, J. (1986). Breakup of Australia and Antarctica estimated as mid-Cretaceous (95±5
748 Ma) from magnetic and seismic data at the continental margin. *Earth and Planetary*
749 *Science Letters*, 77(1), 91-99.
- 750 Veevers, J., & Johnstone, M. (1974). Comparative stratigraphy and structure of the western
751 Australian margin and the adjacent deep ocean floor. *Initial Reports of the Deep Sea*
752 *Drilling Project*, 27, 571-585.
- 753 Vine, F. J. (1966). Spreading of the ocean floor: new evidence. *Science*, 154(3755), 1405-
754 1415.
- 755 Vine, F. J., & Matthews, D. H. (1963). Magnetic anomalies over oceanic ridges. *Nature*,
756 199(4897), 947-949.
- 757 Willcox, J., & Exxon, N. J. T. A. J. (1976). The regional geology of the Exmouth Plateau.
758 16(1), 1-11.
- 759